4-17-2003

New Protonated Thioborate Glasses in the xH2S + (1 – x)B2S3 Series

Annamalai Karthikeyan
Iowa State University

Chad A. Martindale
Iowa State University

Steve W. Martin
Iowa State University, swmartin@iastate.edu

New Protonated Thioborate Glasses in the xH2S + (1 – x)B2S3 Series

Abstract

A new series of anhydrous protonated chalcogenide glasses, xH2S + (1 – x)B2S3, analogous to alkali-modified glasses, have been prepared. The preparation of these glasses was carried out in multiple steps. First crystalline *meta*-thioboric acid, *c*-(HBS2)3, was prepared from vitreous boron sulfide, *v*-B2S3. *c*-(HBS2)3 was then used as a precursor for protonation to prepare a series of xH2S + (1 – x)B2S3 samples with $0.0 \leq x \leq 0.5$. The glass formation region of this system was found to be $0.0 \leq x \leq 0.25$. The density and glass-transition temperature (Tg) of the samples were measured. While a substantial decrease in Tg of the protonated glasses has been observed, there are insignificant changes in the density of the glasses. The IR and NMR spectra of the samples in the region $0.0 \leq x \leq 0.5$ suggest that no tetrahedral borons are formed with the incorporation of protons. The characterization shows that these materials are unique and exhibit no borate anomaly as in the alkali-modified glasses.

Disciplines

Ceramic Materials | Materials Science and Engineering | Physical Chemistry

New Protonated Thioborate Glasses in the xH$_2$S + (1 − x)B$_2$S$_3$ Series

Annamalai Karthikeyan, Chad A. Martindale, and Steve W. Martin*

Department of Materials Science and Engineering, Iowa State University of Science and Technology, Ames, Iowa 50011

A new series of anhydrous protonated chalcogenide glasses, xH$_2$S + (1 − x)B$_2$S$_3$, analogous to alkali-modified glasses, have been prepared. The preparation of these glasses was carried out in multiple steps. First crystalline *meta*-thioboric acid, c-(HBS$_2$)$_3$, was prepared from vitreous boron sulfide, v-B$_2$S$_3$. c-(HBS$_2$)$_3$ was then used as a precursor for protonation to prepare a series of xH$_2$S + (1 − x)B$_2$S$_3$ samples with $0.0 \leq x \leq 0.5$. The glass formation region of this system was found to be $0.0 \leq x \leq 0.25$. The density and glass-transition temperature (T_g) of the samples were measured. While a substantial decrease in T_g of the protonated glasses has been observed, there are insignificant changes in the density of the glasses. The IR and NMR spectra of the samples in the region $0.0 \leq x \leq 0.5$ suggest that no tetrahedral borons are formed with the incorporation of protons. The characterization shows that these materials are unique and exhibit no borate anomaly as in the alkali-modified glasses.

Introduction

Glassy polymeric networks support fast ionic conduction (FIC) of different cations (Li$^+$, Na$^+$, Ag$^+$, etc.).[1,2] Likewise, fast protonic conduction (FPC) is also known in glassy and in polymeric materials.[1,3] However, the actual conducting species in these fast protonic conductors (FPCs) is the hydronium ion (H$_3$O$^+$) and not the bare proton (H$^+$). Hence, the conductivity of these materials depends on the extent of hydration, and such electrolytes are therefore limited to temperatures below ∼150 °C. Electrochemical applications of these hydrated FPCs have inherent difficulties such as methanol crossover, mechanical instability, and limited temperature range (<100 °C). Some of these difficulties can be overcome by synthesizing FPC materials in an anhydrous form. For example, the metal (Me) hydrogen sulfate (or selenate) (X) compounds of the family MeH(XO$_4$) are anhydrous compounds and exhibit FPC.[4,5] The conducting species in this family of FPCs is the H$^+$ ion. However, these materials are oxide-based crystalline materials and require a high-temperature phase for proton conduction. Protonic conductivity is also found in several layered oxides (e.g., HUP, hydrogen uranyl phosphate) and heteropolyacids (PWA, phosphorus tungstic acid).[1,3] In these materials, it is not known clearly whether the mobile species is H$^+$ or H$_3$O$^+$. Further, application of these materials is restricted to temperatures <40−60 °C. Thus it is important to look for alternate materials in an anhydrous form with good thermal and mechanical stability, and chacogenides are promising hosts for high protonic conductivity.

We and others have shown that the sulfide analogue of the oxide-based FIC glasses can also be synthesized[6,7] and have shown that they have better ionic conductivity due to weaker Columbic interactions between sulfide anions and the mobile cation. Hence, these chalcogenide glasses hold much promise as host materials for FPC in an anhydrous form. However, little effort has been made to date to study the protonation of these chalcogenide glasses because of the difficulties in the synthesis and handling of them. These protonated chalcogenide glasses may be better alternatives for hydrated electrolytes in fuel cell applications when FPC is achieved.

We have recently developed a new method to prepare *meta*-thioboric acid.[8] Using this solid acid as a precursor for protonation, we have prepared protonated thioborate glasses, glass-ceramics and polycrystals, in the series xH$_2$S + (1 − x)-B$_2$S$_3$, where $0.0 \leq x \leq 0.5$. In the present paper, we report the details of protonation of v-B$_2$S$_3$ with H$_2$S and the characterization of the resulting materials.

Experimental Methods

Preparation. Vitreous boron sulfide (v-B$_2$S$_3$) was first prepared directly from the elements using the procedure developed in this laboratory.[9] This reaction was carried out at 850 °C in a carborized and sealed under vacuum silica tube and yields v-B$_2$S$_3$ with very little oxide contamination (<1%). The v-B$_2$S$_3$ was then reacted with H$_2$S in the vapor phase, and polycrystalline *meta*-thioboric acid (HBS$_2$)$_3$ was obtained as a vapor condensate. The reaction was carried out in a helium-filled glovebox with negligible oxygen and water contamination (O$_2$ < 1 ppm and H$_2$O < 3 ppm). The details of (HBS$_2$)$_3$ preparation are reported elsewhere.[8]

The polycrystalline *meta*-thioboric acid could not be quenched to a glass owing to the terminated ring structure of the *meta*-thioboric acid (HBS$_2$)$_3$, as shown in Figure 1. To study glass formation in the binary xH$_2$S + (1 − x)B$_2$S$_3$ system, v-B$_2$S$_3$ was added to (HBS$_2$)$_3$ according to the following reaction scheme:

$$2x\text{HBS}_2 + (1 − 2x)\text{B}_2\text{S}_3 \rightarrow x\text{H}_2\text{S} + (1 − x)\text{B}_2\text{S}_3 \quad (1)$$
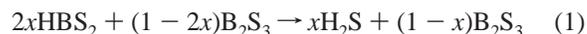
Reactions were carried out for x = 0.1, 0.2, 0.25, 0.33, 0.4, and 0.45. Powdered *meta*-thioboric acid was mixed with a finely ground powder of pure v-B$_2$S$_3$ (∼98% to 99%) and the mixture was loaded into a well-dried silica tube. The silica tube was then sealed under vacuum. The silica tube was carbon-coated for B$_2$S$_3$-rich compositions (x = 0.1 and 0.2) to avoid silica

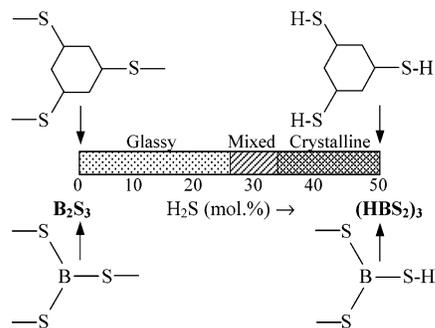* To whom correspondence should be addressed. Tel: (515)-294-0745. Fax: (515)-294-5444. E-mail: swmartin@iastate.edu.

New Protonated Thioborate Glasses

J. Phys. Chem. B, Vol. 107, No. 15, 2003 **3385**

Figure 1. Glass-formation region in the $H_2S-B_2S_3$ system and the structural species involved in the end compositions.

Figure 2. Density and molar volume of samples prepared in the $xH_2S + (1 − x)B_2S_3$ system as a function of H_2S content (x).

contamination in the product. The sealed tube was heated slowly at the rate of 2 °C/min to 150 °C and held there for an hour. It was then heated to 400−450 °C, depending on composition, at the rate of 2 °C/min. The molten mixture was then held at this temperature for an hour. The sealed tube with melt was then quenched in cold water (in air for the B_2S_3-rich compositions) to form the glassy phase. The sealed tube was then opened in the glovebox and the samples were stored in airtight containers.

Characterization of the Materials. The samples prepared were characterized by various techniques. The density of the samples was measured by the Archimedean method using dry kerosene as medium. Three independent measurements were made, and the results were averaged. The error estimates in these measurements were about ±0.02 g/cm³. The glass-transition temperature of the samples was determined using a Perkin-Elmer Pyris-1 differential scanning calorimeter. The IR spectra of the samples were obtained using a Bio-Rad FTS-40 FT-IR spectrometer on KBr pellets with a 5:100 ratio of sample to KBr. The Raman spectra of the powdered samples were obtained using a Bruker RFS 100/S FT-Raman spectrometer using a Nd: YAG 1064 cm⁻¹ laser and a LN₂-cooled Ge detector in a 180° backscattering geometry. The static ¹¹B NMR experiments were performed at a resonance frequency of 64.0179 MHz in a 4.7 T superconducting magnet. The spectra were acquired using a home-built spectrometer. Scans were taken every 5 s, and the data acquisition was taken from the free induction decay (FID) following a π/8 pulse sequence.

Results

Pure v-B_2S_3 is normally obtained as a mild olive-green glass. The incorporation of protons in the glass changed the color systematically toward a bluish gray color and finally to white for the polycrystalline *meta*-thioboric acid composition. The samples in the composition range $0.0 \leq x \leq 0.25$ (or $0.0 \leq y \leq 0.5$) were glassy. The HBS_2-rich samples, $x = 0.4$ and 0.45, had a ceramic texture and were polycrystalline. The sample with $y = 0.33$ was obtained as a mixed glass−ceramic compound. The compositional dependence of the phases obtained is shown in Figure 1. The maximum protonation of the glassy phase was achieved for the sample with $x = 0.25$. Further increase in proton concentration (H_2S content) lead to a glass−ceramic or ceramic phase.

The densities and molar volumes of all of the samples are shown in Figure 2. The addition of H_2S to the B_2S_3 glass marginally decreases the density by about 3%. However, the molar volume decreases by about 40% when the H_2S content in the glass is increased from 0.0 to 50 mol %. This presumably arises because the proton is an elementary particle and its radius and mass are negligible compared to other ions (B^{3+} and $S^{2−}$) present in the phase. As will be seen below in the IR, Raman,
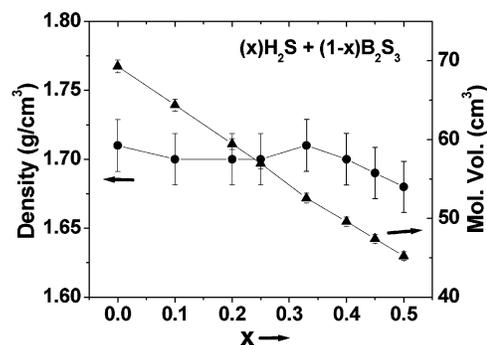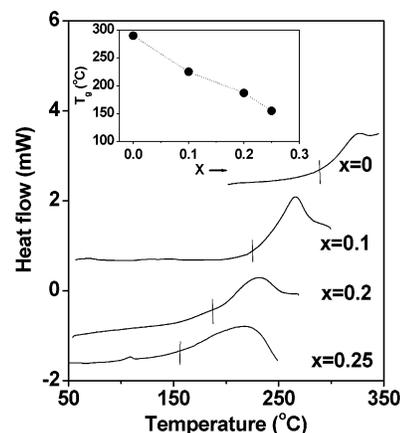

Figure 3. DSC thermogram of the glassy samples obtained in the $xH_2S + (1 − x)B_2S_3$ system, $0.0 \leq x \leq 0.25$. The inset in this figure shows the variation of glass-transition temperature (T_g) as a function of H_2S content (x) in the sample.

and NMR spectra, the addition of protons to the glassy network creates nonbridging sulfur (NBS) atoms, and this may account for the marginal decrease in density. In alkali-modified borate glasses, the density increases significantly (when $0.0 \leq x \leq 0.25$) and thereafter decreases in lighter alkali systems (K, Na)[10,11] and continuously increases in the heavier systems (Rb and Cs).[12,13] In the alkali-modified glasses, the increase in density is caused by the conversion of trigonal to tetrahedral borons. The molar volume of the samples (glassy and polycrystalline), shown in Figure 2, decreases by $\sim$ 40% with the incorporation of 50 mol % of H_2S into the structure. This compositional dependence is almost linear and extends toward the molar volume of pure H_2S (l). This indicates that although the addition of protons to the B_2S_3 network creates NBS atoms, they do not influence a change in the volume of the host material (B_2S_3 glass). Rather, the protons essentially use the available free volume. Further, most of the volume of these materials lies in the sulfur atoms rather than the boron or hydrogen atoms. The substitution of B_2S_3 by H_2S reduces the sulfur content, and hence the molar volume decreases. However, its contribution to total volume and mass remains dominant and hardly changes until $x = 0.5$ (for example, mass contribution is about 82% in B_2S_3 and 84% in HBS_2) and hence the observed trends in density.

The DSC thermograms of the glassy samples are shown in Figure 3. The glass transition temperature (T_g) of pure B_2S_3 is $\sim$ 290 °C. From Figure 3, it can be seen that the glasses with lower H_2S contents ($x = 0.1, 0.2$) have good thermal stability up to 200 °C and have well-behaved thermograms with a glass-transition temperature of 225 and 187 °C, respectively. The T_g dependence on H_2S content in the glass is shown in the inset in
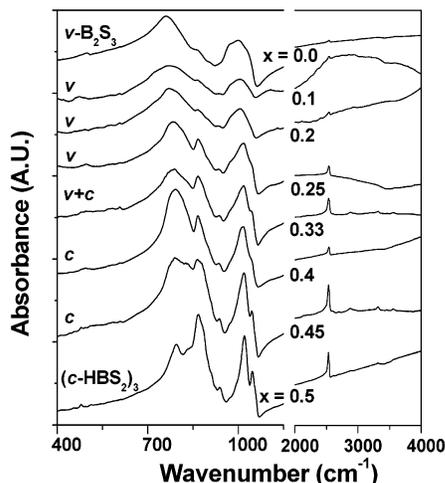
Figure 4. The IR spectra of the samples studied in the $x\text{H}_2\text{S} + (1 - x)\text{B}_2\text{S}_3$ series, $0.0 \leq x \leq 0.5$ (v = vitreous phase; c = crystalline phase; $v+c$ = mixed phase).

Figure 5. The IR and Raman spectra of v-B_2S_3 and the IR and Raman spectra of c-$(\text{HBS}_2)_3$. The Raman spectrum of v-B_2S_3 was obtained from M. Royle et al.[15]

Figure 3. The glass with maximum protonation ($x = 0.25$) shows a reasonably good DSC thermogram with a T_g of ~155 °C. The glass-transition temperature decreases significantly with the addition of H_2S to B_2S_3 glass. These values, though, are considerably higher than the usual functional temperature of the hydrated proton conductors. It is interesting to note that the network breakdown caused by the addition of H_2S, by creating NBS bonds, has a pronounced effect on glass-transition temperature of the glasses.

The IR spectra of the samples in the series $x\text{H}_2\text{S} + (1 - x)\text{B}_2\text{S}_3$ are given in Figure 4. The H−S stretching band observed around 2532 cm^{-1} indicates the presence of anhydrous protons in the materials.[14] In addition, no O−H vibrational mode was observed in the samples, and this further confirms the anhydrous nature of the samples. The intensity of the peak observed at 2532 cm^{-1} increases with the amount of protons incorporated in the glass as expected. This frequency is lower than the S−H stretching frequency of 2560−2620 cm^{-1} observed in organic thiols. This is probably due to the heavier thio-boroxol ring unit attached to the thiol (−SH) versus lighter alkyl and aryl groups. The IR spectra of all of the samples show two dominant vibrational modes, one centered around 1000 cm^{-1} and the other around 760 cm^{-1}. As the H_2S content in the glass increases, these peaks shift slightly toward higher wavenumbers. At higher H_2S contents, when the composition approaches *meta*-thioboric acid ($x = 0.5$), the bands at 760 and 1000 cm^{-1} are split. The band at 770 cm^{-1} is split with peak intensities at 792 and 866 cm^{-1}, and the band at 1000 cm^{-1} is split to 1020 and 1044 cm^{-1}. The IR spectra also show a weak absorption band centered around 1300 cm^{-1}, and this is due to the slight oxide contamination in the starting materials (namely, B_2O_3 in v-B_2S_3). However, this contamination was estimated to be less than a few percent, much lower than that compared to the samples prepared by other procedures.[9] No signature of tetrahedral borate (700 cm^{-1}) and four-membered rings (1200 cm^{-1}) are found in the IR spectra of all the samples.

While *meta*-thioboric acid (c-HBS_2) gives a good Raman spectrum,[8] the Raman spectrum of all other samples could not be recorded with the spectrometer used due to the effects of heating and fluorescence. The Raman and IR spectra of v-B_2S_3 glass and c-$(\text{HBS}_2)_3$ are shown in Figure 5. The Raman spectrum of v-B_2S_3 shown in this figure was obtained from our previous work[15] at 413 nm excitation. It can be seen from the figure that many of the vibrational modes are both IR- and Raman-active.
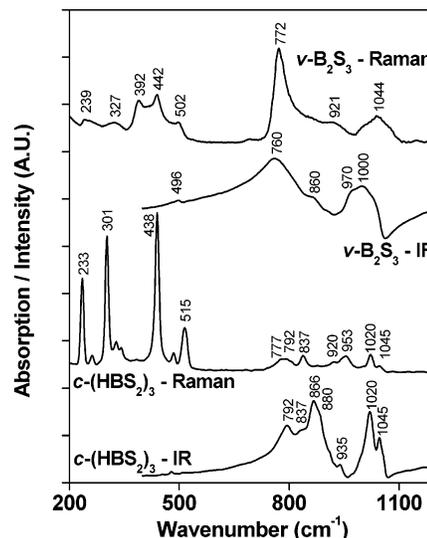
On the basis of the sharing of the vibrational modes and the previous study of the IR and Raman spectra analysis of v-B_2S_3 and alkali-borate glasses,[15−17] the band at 1000 cm^{-1} is assigned to vibrational modes of six-membered rings ($\text{B}_3\text{S}_3\text{S}_{3/2}$) and the band at 770 cm^{-1} is assigned to vibrational modes of trigonal units ($\text{BS}_{3/2}$). The active vibrational modes obtained from symmetry analysis of the six-membered rings and trigonal units are listed in Table 1. According to this analysis, there should be two E′ vibrations of the $\text{BS}_{3/2}$ units and five E′ vibrations of the $\text{B}_3\text{S}_3\text{S}_{3/2}$ units shared between IR and Raman spectra of the v-B_2S_3. From Figure 5, it is clear that the peak observed around 760 cm^{-1} is shared (observed at 772 cm^{-1} in the Raman spectra). The asymmetry of this Raman band on the higher wavelength side indicates that more than one vibrational mode is convoluted into this band. Deconvolution of this peak indicates that the second mode is centered around 800 cm^{-1}. Similarly, the very broad nature of the IR band at 760 cm^{-1} (640−840 cm^{-1}) indicates that at least one vibrational mode on either side of this peak at around 730 and 800 cm^{-1} is convoluted into this broad band as well. Thus, the vibrational mode observed at 800 cm^{-1} is also shared and could be the second E′ mode of the $\text{BS}_{3/2}$ units. The IR band observed around 730 cm^{-1} is assigned to the IR active A_2'' vibrational mode in the trigonal units.

The Raman band observed at 1044 cm^{-1} is very broad and is uncharacteristic of Raman peaks.[15] This broadening might be associated with closely spaced vibrational energy levels. Hence, this band is assigned to the 5E′ modes of the $\text{B}_3\text{S}_3\text{S}_{3/2}$ rings. As shown in the figure, these modes are also shared in the IR spectrum, however at a slightly lower wavelength of 1000 cm^{-1}. The IR peak observed at 970 cm^{-1} of v-B_2S_3 is not seen in the Raman of v-B_2S_3, and hence it is assigned to the A_2'' vibrational modes of the thioboroxyl rings. The Raman-only active modes (A_1' modes) are observed at 500 cm^{-1} and below. On the basis of the previous reports,[15−17] the Raman peaks observed at 502, 442, and 239 cm^{-1} are assigned to the A_1' modes of the ring structure. The other less-intense peaks and shoulders arise due to structural contamination in the sample. However, it is still not clearly known whether the peaks at 239 and 327 cm^{-1} are due to A_1' mode and structural impurities, respectively, or vice versa. The peak at 392 cm^{-1} was found to lose its intensity with Na_2S content in the sodium borate

New Protonated Thioborate Glasses

J. Phys. Chem. B, Vol. 107, No. 15, 2003 **3387**

TABLE 1: Active Vibrational Modes in Different Structural Units

structural unit	infrared	Raman	both
six-membered ring $B_3S_3S_{3/2}$	$2A_2''$	$3A_1'$	$5E'$
trigonal units $BS_{3/2}$	A_2''	A_1'	$2E'$
protonated trigonal unit $BS_{2/2}SH$			B–S stretch–all A, B modes; S–H stretch–A_1 mode

glasses[15] and hence must be due to the Raman-only active A_1' mode in the trigonal $BS_{3/2}$ units.

As shown in Figure 4, when H_2S is added to v-B_2S_3, the strong IR peak observed at 760 cm^{-1} loses its intensity and shifts toward higher frequency. In crystalline *meta*-thioborate, c-$(HBS_2)_3$, it is observed at 792 cm^{-1}. The shoulder observed at 866 cm^{-1} gains intensity rapidly with increase in H_2S content. Hence, it must be due to the protonated species, namely, the trigonal $BS_{2/2}SH$ units. This 866 cm^{-1} mode is also observed as a very weak peak in v-B_2S_3 and indicates the proton contamination present in the starting material.[9] This is also ascertained by the weak S–H stretching mode observed at 2532 cm^{-1} in v-B_2S_3. The rings modes centered around 1000 cm^{-1} in the IR spectrum of v-B_2S_3 also shift toward higher frequency and split up. In c-HBS_2, it is observed as a doublet (probably even a triplet when the asymmetry of the peak at lower wavelength side is taken into account) with peaks at 1020 and 1045 cm^{-1}. In addition to these major changes in the IR spectra, a small peak is also found to grow around 940 cm^{-1} with the increase in H_2S content in the sample. The assignments for the protonated samples were done on the basis of the comparison of IR and Raman spectra of c-HBS_2 and those of v-B_2S_3 as described below.

The IR and Raman spectra of c-HBS_2 are shown in Figure 5. A comparison of these two spectra indicates clearly that they are richer than those for v-B_2S_3 and more peaks are shared than are in v-B_2S_3. According to the symmetry analysis of planar trigonal units (D_{3h} symmetry), the total number of shared ($2E'$) and IR-only active (A_2'') modes is three. At least four peaks and two shoulders are seen in the IR spectrum of c-HBS_2 in the band starting from 750 to 950 cm^{-1}, which arise because of trigonal ($BS_{2/2}SH$) units. This is explained as follows. The addition of H_2S to B_2S_3 creates NBS, and the $BS_{3/2}$ units are converted to $BS_{2/2}SH$ units with the proton covalently bonded to the sulfur atom. This changes the symmetry of the unit from D_{3h} to C_{2v}, and the degeneracy of the E$'$ modes is lost. Each E$'$ mode is split into two, and now there are four E$'$ modes, and all are shared modes. The peaks observed at ~792, 837, and 935 cm^{-1} and the shoulder observed at ~880 cm^{-1} are all assigned to the E$'$ modes. The new peak observed at ~953 cm^{-1} in the Raman spectra of c-HBS_2 is due to the A_2'' mode of the $BS_{2/2}SH$ units because it becomes active when its symmetry changes to C_{2v}. In the IR spectra, it is observed at ~866 cm^{-1}. Our recent far-IR (FIR) spectroscopy investigation of a Ag_2S + B_2S_3[18] system shows that the Raman peaks observed below 500 cm^{-1} are also present in the far-IR spectra and supports the hypothesis that symmetry of the trigonal unit has changed to C_{2v}. Hence, all of the vibrational modes are both Raman and IR active.

The symmetry of the six-membered rings in c-HBS_2 does not change because all of the external sulfur atoms in this structure are terminated with protons. The $BS_3S_{3/2}$ ring unit in the pure v-B_2S_3 changes to the $B_3S_6H_3$ (or $(HBS_2)_3$) terminated ring in c-HBS_2, but the symmetry is preserved. However, in the intermediate compositional range, especially in the glass-forming region, structural units such as $(B_3S_3)S_{1/2}S_2H_2$ or $(B_3S_3)S_{2/2}SH$ are possible. Hence, these different units may have different symmetry elements, but their energy levels may remain closely spaced. The IR bands of the samples in this composi-

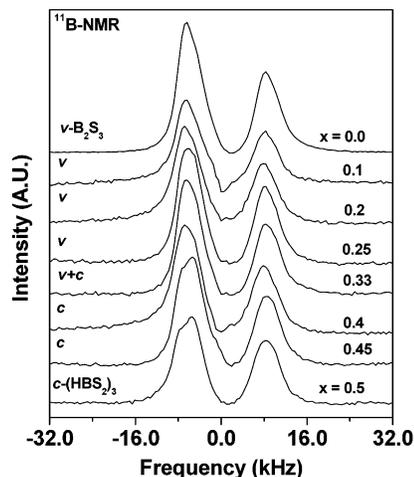**Figure 6.** The static ^{11}B NMR spectra of the samples studied in the $xH_2S + (1 − x)B_2S_3$ series, $0.0 ≤ x ≤ 0.5$ (v = vitreous phase; c = crystalline phase; $v+c$ = mixed phase).

tional range are very broad, and it is difficult to deconvolute the individual peaks. As noted earlier, the IR bands shift toward higher wavenumbers when protons are added to the external sulfur atoms in the ring structure. In c-HBS_2, this band is split with peak intensities at 1020 and 1045 cm^{-1}. These modes are also Raman-active, as expected.

The Raman spectrum of c-HBS_2 shows four strong and narrow peaks at lower wavenumbers. The peaks observed at 233, 438, and 515 are due to Raman-active 3A$'$ modes of the six-membered rings. They are observed at 239, 442, and 502 cm^{-1} in v-B_2S_3, respectively. The 392 cm^{-1} peak observed in the Raman spectra of v-B_2S_3 is not seen in c-HBS_2; however, a new peak appears at 301 cm^{-1}. This suggests that the 301 cm^{-1} peak could be due to the A_1' mode of the trigonal unit. The change in symmetry triggers this shift in peak position. All of the other less-intense peaks observed at lower wavenumbers (<500 cm^{-1}) are due to the structural contamination in the sample. Symmetrical modes of low energies, like those mentioned above, are characteristic of chalcogenide materials with ring and chain structures. For example, the strong Raman mode observed at 438 cm^{-1} is due to the symmetric stretch of the sulfur atom in the thio-boroxol rings. The structural units present in the end compositions ($x = 0.0$ and 0.5), obtained after the IR and Raman analysis, are given in Figure 1. The samples in the intermediate compositional regime will have a combination of these structural units.

NMR measurements were carried out to study the coordination geometry of the borate units. The ^{11}B NMR spectra of all of the samples (glassy and crystalline) are shown in Figure 6. The ^{11}B NMR shows two resonance peaks, one at 8.3 kHz (128 ppm with respect to boric acid) and the other at −6.5 kHz (−104 ppm). These two resonance peaks are characteristic of boron in planar triangular geometry ($BS_{3/2}$ units).[19,20] No signature of tetrahedral borate units is observed in the NMR spectra. This is also consistent with the structural information obtained from IR and Raman spectra. A closer observation of the ^{11}B NMR spectra reveals that the peak at −6.5 kHz (−104 ppm) is actually made up of two closely spaced resonance peaks, one at −6.5 kHz (−104 ppm) and an another −5.4 kHz (−84 ppm). This

behavior of ^{11}B spectra shows that there are two different trigonal boron sites. At lower H_2S content, in the glassy compositional region, the satellite resonance peak at -5.4 kHz appears as a shoulder, and with the increase in B_2S_3 content, this resonance peak gains intensity. This compositional dependence implies that the resonance peak at -5.4 kHz (-84 ppm) is due to the trigonal boron units with attached protons ($BS_{2/2}SH$ units). In c-HBS_2, the resonance peak at -5.4 kHz overshadows the resonance peak originally observed at -6.5 kHz, as expected.

Discussions

The present investigation has revealed that it is possible to incorporate H_2S in the B_2S_3 network in a manner analogous to the $M_2X + B_2X_3$ systems, where, M = Li, K, Na, Cs, Rb, or Ag and X = S or O. The spectroscopic investigations clearly suggest that the H_2S plays a role similar to metal sulfides or oxides (M_2X) by creating nonbridging sulfur atoms. However, unlike alkali borate and thioborate glasses, no anomalous structural effects such as change in coordination of the borate unit (from trigonal to tetrahedral unit) or density variations are observed. The addition of H_2S depolymerizes the borate network and creates two NBS atoms by forming two $-S-H$ bonds. The $-S-H$ bonds formed here are covalent and are different from the partial covalent (to ionic) bonding seen in alkali borate glasses with $-S-M$ bonding.

The glass-formation region is found to be $0 \leq x \leq 0.25$. This compositional range is also consistent with the structural information obtained from the spectroscopic studies. The c-HBS_2 ($x = 0.5$) is obtained as a molecular solid and is predominantly made of six-membered rings with terminal protons. The polymeric network essential for the formation of glassy phase can be achieved only if the NBS atoms in c-$(HBS_2)_3$ are converted to bridging sulfur (BS). There are three NBS atoms in c-$(HBS_2)_3$, and converting one of these NBS to a BS atom (($B_3S_3)S_{1/2}S_2H_2$ unit or $x = 0.4$) will provide one external linkage to a similar ($B_3S_3)S_{1/2}S_2H_2$ unit but still cannot provide a long-range network. Hence, at least two BS atoms are required for glass formation. The corresponding structural unit, which provides the long-range polymeric network, is ($B_3S_3)S_{2/2}SH$. This is equivalent to $25\%H_2S + 75\%B_2S_3$ (or $x = 0.25$). Beyond this composition ($0.25 \leq x \leq 0.4$), the glass-forming ability decreases rapidly and the sample is obtained as a mixed-phase or crystalline compound. There are also some trigonal units presents in the structure, and they improve the glass-formation ability. The thio-boroxol rings found in v-B_2S_3 and in crystalline c-$(HBS_2)_3$ are very stable under controlled atmosphere. The heat treatment of c-$(HBS_2)_3$ beyond the melting point released H_2S gas and yielded v-B_2S_3. Spectroscopic analysis of the various heat-treated samples show that the dominant and stable structural unit is the six-membered thio-boroxol ring, like those in oxy-borate glasses and in boric acid. However, different kinds of rings found in oxy-borate glasses are not seen in thio-borates.

The densities of the glasses and other crystalline samples in the protonated series do not vary much from that of the host material (density of v-$B_2S_3 = 1.70$ g/cm^3) where only about a 3% decrease in density is observed. Addition of H_2S (solid density $= 1.12$ g/cm^3) creates two NBS atoms, and the protons are bonded to NBS by covalent bonding. In the present system, protonation does not alter the basic coordination geometry, and the borate units are in planar trigonal geometry. The trigonal geometry formed by sp^2 hybridization of the boron atoms has a $S-B-S$ bond angle of $120°$. The six-membered ring units (sp^2 hybridization in sulfur atoms) has a $B-S-B$ bond angle of $120°$. If the sulfur atoms provide a pure p bonding, one would

expect a $S-B-S$ bond angle close to $90°$. However, spectroscopic studies reveal that six-membered ring units dominate the structure. Protons are bonded to the external sulfur atoms in these rings. On the basis of the highly directional property of the proton bonding, we realize that the $B-S-H$ bond angle is also close to $120°$. The formation of NBS atoms and structural modification caused by lower density H_2S are expected to decrease the density of the sample upon protonation. However, the density remains more or less constant. Considerable reorganization of the network by altering the interborate linkages would have occurred to maintain the density constant. It should be noted that these structural changes have an enhanced effect on glass-transition temperature (T_g). The glasses and other polycrystalline samples prepared here have unique physical and structural properties. The present study of new $H_2S-B_2S_3$ glasses opens a new choice for glass–ceramic research.

The glasses in the series $M_2X + B_2X_3$ exhibit good ionic conductivity; however, in the $H_2S + B_2S_3$ glasses, the covalency of $H-S$ bonding will have greater role in limiting its conductivity. This is also evident from the higher electronegativity of the H atom (~ 2.0) compared to other metal (M) atoms (≤ 1.0) owing to the poor nuclear screening constant of H atom. Hence, the long-range migration of proton necessitates an additional supporting mechanism like structural reorganization followed by an ion jump or vice versa. These requirements can possibly be met by modifying the structure of the binary glasses by creating either a rotator phase or disordered cation sublattice. Structural modification of the protonated borate glasses and conductivity measurements of these materials are being performed and will be reported elsewhere.

Conclusions

Crystalline *meta*-thioboric acid has been used to prepare a series of $H_2S-B_2S_3$ glasses and glass–ceramic and crystalline materials. While the density of these glasses remains practically unaffected, the glass-transition temperature was found to decrease significantly with the addition of hydrogen sulfide to thioborate. The IR and Raman investigations suggest that that these glasses are comprised of trigonal borate units and six-membered rings. Unlike other alkali-modified borate glasses, no tetrahedral groups upon addition of H_2S to B_2S_3 are formed. The ^{11}B NMR spectra are also consistent with the three-fold coordination of borate units. The material prepared here shows that it is possible to protonate chalcogenide glasses in an anhydrous form and provides a new choice for investigation in chalcogenide glass–ceramic materials toward the development of anhydrous acids with fast protonic conductivity.

References and Notes

(1) *Superionic Solids and Solid Electrolytes: Recent Trends*; Laskar, A. L., Chandra, S., Eds.; Academic Press Inc.: Boston, MA, 1989.

(2) *Hand Book of Solid State Batteries and Capacitors;* Munshi, M. Z. A, Ed.; World Scientific: Singapore, 1995.

(3) Alberti, G.; Casciola, M. *Solid State Ionics* **2001**, *145*, 3–16.

(4) Baranov, A. I.; Tregubchenko, A. V.; Shuvalov, L. A.; Shchagina, N. M. *Sov. Phys. Solid State* **1987**, *29*, 1448–1449.

(5) Pawlowski, A.; Pawlaczyk, Cz.; Hilczer, B. *Solid State Ionics* **1990**, *44*, 17–19.

(6) Martin, S. W. *J. Am. Ceram. Soc.* **1991**, *74*, 1767–1784.

(7) Angell, C. A. *Chem. Rev.* **1990**, *90*, 523–542.

(8) Karthikeyan, A.; Martindale, C. A.; Martin, S. W. *Inorg. Chem. Commun.* **2002**, *41*, 622–624.

New Protonated Thioborate Glasses

J. Phys. Chem. B, Vol. 107, No. 15, 2003 **3389**

(9) Martin, S. W.; Bloyer, D. R. *J. Am. Ceram. Soc.* **1990**, *73*, 3481−3485.

(10) Martin, S. W.; Cho, J.; Polewik, T.; Bhowmik, S. *J. Am. Ceram. Soc.* **1995**, *78*, 3329−3335.

(11) Cho, J.; Martin, S. W. *J. Non-Cryst. Solids* **1995**, *190*, 244−250.

(12) Cho, J.; Martin, S. W. *J. Non-Cryst. Solids* **1996**, *194*, 319−325.

(13) Cho, J.; Martin, S. W. *Phys. Chem. Glasses* **1996**, *37*, 155−159.

(14) Gates, A. S.; Edwards, J. G. *Inorg. Chem.* **1977**, *16*, 2248−2252.

(15) Royle, M.; Cho, J.; Martin, S. W. *J. Non-Cryst. Solids* **2001**, *279*, 97−109.

(16) Royle, M.; Cho, J.; Martin, S. W. *J. Am. Ceram. Soc.* **1993**, *76*, 2753−2759.

(17) Cho, J.; Martin, S. W. *J. Non-Cryst. Solids* **2002**, 298, 176−192.

(18) Mei, Q.; Schrooten, J.; Meyer, B.; Saienga, J.; Martin, S. W. *J. Non-Cryst. Solids*, submitted for publication, 2002.

(19) Sills, J. A.; Martin, S. W.; Torgeson, D. R. *J. Non-Cryst. Solids* **1994**, *168*, 86−96.

(20) Sills, J. A.; Martin, S. W.; Torgeson, D. R. *J. Non-Cryst. Solids* **1994**, *175*, 270−277.